Preliminary Analysis of Nonlinearity in F/A-18E/F Noise Propagation

Kent L. Gee*, Thomas B. Gabrielson†, Anthony A. Atchley‡, and Victor W. Sparrow§
The Pennsylvania State University, University Park, PA, 16802

Analyses of recent F/A-18E/F military power and afterburner measurements suggest that the noise propagation is nonlinear in the far field. Spectral broadening takes place as the radiated noise propagates from 18 to 150 m, the limits of the measurement range. This broadening phenomenon cannot be readily explained in terms of linear propagation effects. Calculation of a nonlinearity indicator derived by Howell and Morfey supports the assertion that nonlinear propagation effects are present. Furthermore, skewness and kurtosis calculations indicate that the noise data distributions are non-Gaussian over the propagation range at these engine settings. Finally, the measured spectra have been compared against predictions obtained with existing nonlinear spectral evolution methods. Even though the prediction results compare poorly with the actual measurements, this is attributable to limitations of the spectral evolution methods themselves.

I. Introduction

THIS paper contains a preliminary analysis of F/A-18E/F Super Hornet static engine run-up noise measurements made at NAVAIR Lakehurst, NJ on 15 April 2003. Results of the analysis show evidence of nonlinear acoustic propagation effects. These effects are typified by a spectral broadening in which energy is transferred from mid-frequencies to the ends of the spectrum. The evolution of a finite-amplitude noise spectrum may be explained in terms of two time-domain phenomena. Waveform steeping is responsible for the transfer of energy from mid to high frequencies, whereas shock coalescence and a corresponding increase in time scale accounts for a relative increase of energy at low frequencies[1]. In this paper, the measurement setup and apparatus as well as analysis procedure are first described. Next, the probability density function (PDF) and related statistical quantities are calculated. The measured spectra are compared with linear predictions, which take into account spherical spreading and atmospheric absorption, as well as nonlinear predictions from two existing jet noise prediction schemes[2-4]. The assertion that the disparity between linear predictions and measurements are caused by nonlinear propagation is supported by calculation of a quantity derived by Howell and Morfey as a useful nonlinearity indicator[3].

II. Measurement and Analysis Procedure

Measurements of the F/A-18E/F were made with the engines idling, at military thrust, and with afterburners engaged. These three engine conditions will be abbreviated hereafter as “Idle”, “Mil”, and “AB”. The approximate ambient temperature and relative humidity were 20° C and 30% during the tests. A positive temperature gradient was measured near the ground at 1° C per meter, implying a downward refracting medium. Wind conditions were relatively slight; the average wind speed was approximately 5 knots (3 m/s). Data were acquired at 18, 74, and 150 m (approximately 60, 243, and 493 ft) from the engine nozzles along a radial line 135° from the forward direction. The 18 m data were acquired with a Bruel & Kjaer 4938 ¼-inch condenser microphone flush mounted in an aluminum plate baffle located horizontally on the pavement. The 74 and 150 m data were acquired with handheld Endevco 8510C-15 piezoresistive pressure transducers held approximately 1.2 m (4 ft) above the ground. Pre- and

* Ph.D. Candidate, Grad. Prog. in Acoustics, Penn State Univ., 202 Applied Science Bldg., University Park, PA 16802, kentgee@psu.edu, Student Member AIAA
† Senior Research Associate, Applied Research Lab, Penn State Univ., P.O. Box 30, State College, PA 16804
‡ Professor of Acoustics and Chair, Grad. Prog. in Acoustics, Penn State Univ., 217 Applied Science Bldg., University Park, PA 16802, Member AIAA
§ Associate Professor of Acoustics, Grad. Prog. in Acoustics, Penn State Univ., 316B Leonhard Bldg., University Park, PA 16802, Member AIAA

post-measurement sensor calibrations were performed using a Bruel & Kjaer 4228 pistonphone. Time series data were recorded with portable Sony TCD-D8 digital audio tape (DAT) recorders sampling at 44.1 kHz. Average power spectral densities (PSD) were calculated by dividing approximately 12 seconds of data into blocks containing 4096 samples with 50 percent overlap. A Hanning window was applied to each data block and the scaled discrete Fourier transform (DFT) computed. The mean PSD for each measurement was calculated by averaging the magnitude-squared DFT for each data block. Pressure amplitude corrections for the DAT anti-aliasing filter response and sensor diffraction effects were also applied. Because of uncertainty regarding the sensor diffraction corrections at high frequencies, the analyses performed have been limited to below 10 kHz.

III. Results

A. Power Spectral Measurements

In Figs. 1-3 the PSD at the three measurement distances is shown for each of the engine conditions. In Fig. 1, the overall sound pressure levels (OASPL) for AB, Mil, and Idle at 18 m are 151, 147, and 99 dB re 20 µPa, respectively. Because the Idle spectra reaches the system noise floor at approximately 6 kHz, all additional analysis of that data is restricted to below that limit. For the latter two distances, 74 and 150 m, shown in Figs. 2 and 3, the engine idle levels are largely below their respective noise floors and are not meaningful measurements. The irregular nature of the noise floors above 1 kHz in Figs. 2 and 3, which are shown as a noise equivalent PSD, is caused by the amplitude diffraction correction applied to the Endevco sensors. The OASPL at 74 m are 135 and 132 dB re 20 µPa for the AB and Mil engine settings. By 150 m the OASPL for AB and Mil conditions are reduced to 127 and 123 dB re 20 µPa, respectively.

The 74 and 150 m spectral measurements exhibit multiple dips in level of several dB, and while not readily apparent from the logarithmic frequency scale, the dips occur at roughly regular intervals of approximately 600-700 Hz. There is a slight offset of dip frequencies between the AB and Mil measurements at both locations that grows as a function of frequency; however, the dip frequencies for a given engine setting remain fairly consistent between the 74 and 150 m spectra. Some of the mid-frequency dips are less pronounced at 150 m, but the first dip at approximately 700 Hz and those above 5 kHz are still readily distinguishable. The cause of the spectral dips has not been conclusively determined at this point, although they may be attributable to multipath interference due to the sensors' locations above the ground. However, the consistency between dip frequencies at 74 and 150 m would imply that the propagation path length differences for the two measurement locations are nearly the same, which seems unlikely. This suggests that while multipath interference is likely present due to the test configuration, the cause of the spectral dips could be more complex.

B. Statistical Calculations

As part of the data analysis, the probability density function (PDF) for each of the measurement locations and engine conditions was calculated, along with the skewness (S) and kurtosis (K), which are the normalized third and fourth central moments of the probability distribution. The value of S, which is a measure of the asymmetry of the data distribution, has been used to quantify the phenomenon known as crackle[5,6]. No similar physical phenomenon has been associated with K, which describes the peakedness of the PDF. Although calculation of the PDF and other statistical quantities is insufficient by itself as evidence of nonlinear propagation effects, it is very relevant to the discussion of additional analyses described subsequently.

In order to limit all analyses to below 10 kHz, an eighth-order digital lowpass Butterworth filter with a cutoff frequency of 10 kHz was applied to the waveform data before calculating the PDF. In order to only analyze the 18 m Idle data above the system noise floor, the cutoff frequency was set at 6 kHz. Figure 4 shows the calculated PDF for the lowpass-filtered 18 m Idle data. The calculated PDF from the measured data is compared to the PDF for a statistically Gaussian waveform possessing the same mean value and standard deviation. The Idle distribution is nearly Gaussian (S = 0 and K = 3 for Gaussian data), although a slight asymmetry is visible. However, deviations from a Gaussian distribution occur for the AB and Mil engine settings; example results are shown in Figs. 5 and 6 for the AB case at 18 and 150 m, respectively. The statistical results for the various measurement locations and engine settings are summarized in Table 1. The

Table 1. Skewness (S) and kurtosis (K) for the engine conditions and measurement locations.

	S	K
Idle, 18 m	-0.01	3.05
Mil, 18 m	0.38	3.13
Mil, 74 m	0.25	3.25
Mil, 150 m	0.08	2.99
AB, 18 m	0.60	3.40
AB, 74 m	0.39	3.41
AB, 150 m	0.26	3.05

results show that the propagation may be considered non-Gaussian over the measurement range, although the statistics appear to become more Gaussian by 150 m, especially for the Mil power case. This non-Gaussianity has implications with regards to existing nonlinear spectral evolution prediction schemes. Finally, although its physical significance is currently unknown, it is worth noting that K increases between 18 and 74 m for Mil power, and remains essentially constant for the AB case, whereas S decreases for both engine settings over the same range.

IV. Evidence of Nonlinear Propagation Effects

Analysis of the F/A-18E/F data demonstrates evidence of nonlinear acoustic propagation effects. This portion of the analysis takes two forms. First, linear extrapolation of the 18 and 74 m measured spectra to 150 m and comparison with the measured spectrum at that distance shows significant differences between the extrapolated and measured spectra. The evolution of the measured spectra is characteristic of finite-amplitude noise propagation. The second portion of the analysis is the calculation of a nonlinearity indicator derived by Howell and Morfey[2], which strengthens the position that the differences between the measured and extrapolated spectra are caused by nonlinear propagation effects.

A. Comparison of Linear Extrapolation with Measurement

Extrapolation of the 18 and 74 m measured spectra to the 150 m location shows marked differences between the extrapolated spectra and the measured spectrum at that distance for both the Mil and AB cases, shown respectively in Figs. 7 and 8. The extrapolation, equivalent to allowing the spectrum to evolve linearly over the required propagation distance, is carried out by calculating the decrease in power for each frequency bin due to spherical spreading and atmospheric absorption. The absorption model developed by Bass *et al.*[7,8] was used for the extrapolations. Both 18 and 74 m linear extrapolations out to 150 m have been calculated because of potential concern as to whether the geometric far field, where the assumption of spherical spreading becomes valid, has been reached by 18 m. Examination of Fig. 7 for the engine at Mil power shows excess power at high frequencies for the measured spectrum as compared to the extrapolated spectra, a difference of 23 dB from the 18 m extrapolation and 10 dB from the 74 m extrapolation. In addition, there is a depletion of power at mid-frequencies, possibly exaggerated by the spectral dips mentioned previously, and an increase of power at low frequencies. This latter phenomenon is especially true for the 18 m extrapolation, where the peak frequencies of the spectrum shift. This spectral broadening is characteristic of the nonlinear acoustic propagation of high-amplitude noise. The AB results shown in Fig. 8 yield a similar trend with regards to spectral broadening, although the overall levels below 100 Hz are much greater than in the Mil power case.

B. Howell-Morfey Nonlinearity Indicator

In their efforts to develop a prediction method for the nonlinear evolution for a high-amplitude jet noise spectrum, Howell and Morfey derived a first order equation for the evolution of the power spectrum as a function of range that predicts the occurrence of nonlinear propagation effects only if Q_{p^2p}, a third order spectral quantity, is non-zero (see Eq. (5) of Ref. 3). Q_{p^2p} is defined as the imaginary part of the cross-spectral density between the pressure squared and the pressure and may be written as

$$Q_{p^2p}(\omega) = \mathrm{Im}\left(\Im\left\{p^2(t)\right\}\Im^*\left\{p(t)\right\}\right),$$

where $\Im$ and * represent Fourier transform and complex conjugation operators. While the model equation is not useful for prediction purposes because Q_{p^2p}, in general, will vary in an unknown fashion along the propagation path, nonlinear energy transfer at a given location may be readily identified by a nonzero Q_{p^2p} measurement. Howell and Morfey's nonlinearity indicator, a nondimensional ratio dubbed *Q/S*, is derived by normalizing Q_{p^2p} by the power spectrum multiplied by the root-mean-square pressure. McInerny and Olcmen have recently performed *Q/S* calculations to investigate nonlinear propagation effects present in rocket noise[9].

The Howell-Morfey (HM) nonlinearity indicator has the following physical interpretation. For a given frequency, if $Q/S < 0$, energy is being transferred from other frequencies, meaning that the power contained in that frequency bin is increasing. If $Q/S > 0$, energy is being transferred to other frequencies and the amount of power at that frequency is decreasing. If $Q/S = 0$, no interaction between frequency components exists and the propagation is subject only to linear loss mechanisms such as spreading and absorption. In Fig. 9, *Q/S* is plotted from the 18 m

measurements of AB, Mil, and Idle conditions. For the Idle case, no nonlinear propagation should be expected because an OASPL of 99 dB re 20 μPa is certainly within the linear regime. The averaged *Q/*S for Idle approaches zero, meaning that no nonlinear energy transfer is taking place. It should also be pointed out that this *Q/*S could have been predicted from the 18 m Idle PDF in Fig. 4, since odd-order spectra are zero for a statistically Gaussian signal.

Q/S is significantly different for the Mil and AB data in Fig. 9. There are two main frequency regions in which the ratio has opposite signs, indicating nonlinear propagation effects are present. Energy from approximately 60 Hz to 1 kHz is being transferred upward in the spectrum. Because *Q/S* is positive at low frequencies (e.g., below 100 Hz), this suggests that shock coalescence, which should result in a negative *Q/S* at low frequencies, is not yet occurring at 18 m. Although the *Q/S* calculations for 74 and 150 m shown in Fig. 10 suffer from sharp sign changes in the mid-frequency region that appear to be related to the previously discussed spectral dips, there is again evidence of nonlinear energy transfer, this time to both high and low frequencies.

V. Comparison against Existing Nonlinear Spectral Evolution Methods

Long range nonlinear spectral evolution models for high-amplitude jet noise were proposed in the early 1980's, by Crighton and Bashforth[2] (CB) and Howell and Morfey[3,4] (HM), but neither has received significant attention since then. An alternative finite-amplitude spectral evolution method was recently investigated by Menounou and Blackstock[10]; however, their model does not currently incorporate geometrical spreading or absorption due to relaxation effects, and is therefore not readily applicable to jet noise propagation. Because the CB and HM methods are well developed in their original references, their main details are simply summarized below. The CB method is a series expansion solution for the power spectrum, which has its roots in an ensemble-averaged version of the Burgers equation, the simplest nonlinear model equation that includes the effects of nonlinearity and dissipation. In the CB solution, spherical spreading and arbitrary atmospheric absorption are included, and a Gaussian source assumption is made. Because the series solution is truncated after second order, it suffers from range limitations that are amplitude and frequency dependent. However, the method was intended to be valid for distances up to 500 m, which is much greater than the range considered here.

The HM method also begins with a series expansion solution of the Burgers equation for the power spectrum; however, it differs from the CB method in that individual terms of the Taylor series, which consist of derivatives of the power spectrum with respect to range, are equated with terms involving higher order spectra (such as Q_{p^2p} discussed previously), which result from analytically evaluating the derivatives. The outcome is a (potentially infinite) set of ordinary differential equations that can be each used to describe the evolution of the power spectrum as function of range. However, the same difficulty arises with each of the prediction equations as occurred earlier in the discussion of the HM nonlinearity indicator. Each of these higher order spectra varies in an unknown manner along the propagation path and therefore the prediction problem remains insoluble unless these spectra can be written directly in terms of the power spectrum at all range points. This can only be accomplished by means of a quasi-normal hypothesis, which requires that all higher order spectra remain related to the power spectrum in a Gaussian fashion. This assumption yields differential equations that may be readily solved with a simple finite difference scheme.

The equation used for prediction of the power spectral evolution results from the second-order term in the series expansion, which is the first nontrivial model equation under the quasi-normal hypothesis. Like the CB method, a Gaussian source assumption is used at the input. Howell and Morfey reported that empirical modifications to their model equation were required for two reasons; to prevent negative PSD predictions at large distances and for data fitting purposes[3,4]. An extensive investigation of these modifications was carried out and it was found that the modification to prevent a negative value for the PSD was unnecessary but harmless for a sufficiently small range step and that the data fitting modification was not extremely beneficial in any case tested. Nevertheless, the same modifications implemented in the original HM method have been included for the sake of method reproduction in the results that follow.

The CB and HM methods have been evaluated for the Mil power case in Figs. 11 and 12, propagating out to 150 m from 18 and 74 m, respectively. These results are shown alongside the linear extrapolation and measured PSD for the sake of comparison. Neither method reasonably approximates the PSD at 150 m for either of the two starting range points. Both methods appear to converge to the linear prediction below a few hundred Hz; neither predicts any sort of shift of spectral energy to lower frequencies. At high frequencies, the CB method appears to have the same slope as the linear extrapolation, which is principally due to the series expansion form of the solution. The HM results at high frequencies vary substantially from the predictions originally published, in which the nonlinear prediction falls between the linear prediction and the measured spectrum. Use of an extremely large range step yields predictions that are similar to those reported by Howell and Morfey, but algorithm stability is extremely

sensitive to parameter choices. It is likely that, due to a deficiency in computational processing power when the method was developed, a large range step was used to obtain the published results. However, when the published HM method is used to propagate the current data along increasingly fine numerical grids, the predicted spectra converges to those shown in Figs. 11 and 12.

The failure of the CB and HM methods to predict the measured PSD at 150 m does not mean that the differences between measurement and linear propagation theory are not caused by nonlinear propagation effects because it is implausible that either prediction represents physically realistic nonlinear propagation. The results of this evaluation indicate that a method that operates solely on the power spectrum to successfully predict nonlinear spectral evolution is improbable. Both methods are founded on a solid nonlinear acoustics model equation and rigorous mathematical development. However, to reach a solution, restrictive assumptions must be made about the nature of the source and the propagation. The values for the skewness and kurtosis in Table 1 for 18 and 74 m demonstrate that a Gaussian source assumption is likely unwarranted for a nonlinear propagation algorithm applicable to high-amplitude jet noise. Furthermore, the fact that the methods operate on the power spectrum directly means that they neglect signal phase information and therefore a large portion of the actual propagation physics.

VI. Conclusion

A number of analyses performed on F/A-18E/F Mil and AB data demonstrate evidence of nonlinear propagation effects. While effects such as local meteorology and multipath interference need to be more thoroughly investigated, none would appear to sufficiently explain the spectral broadening that occurs between 18 and 74 m and 74 m and 150 m. The attribution of this broadening to nonlinear acoustic effects is strengthened by calculation of the Howell-Morfey nonlinearity indicator, *Q/S*, which by interpretation shows energy being transferred from mid to high frequencies at 18 m and to both low and high frequencies at 74 and 150 m. Evaluation of two existing nonlinear prediction methods with the spectral data demonstrates the need for future development of alternative algorithms that do not neglect phase information or assume a source with Gaussian statistics. This assumption has shown to be unjustifiable, at least for this aircraft at Mil and AB operating conditions, by the calculation of skewness and kurtosis for the various cases. While additional corroborative investigations are required, the inclusion of nonlinear effects appears to be important in the analysis and prediction of F/A-18E/F noise propagation.

Acknowledgments

These measurements would not have been possible without the cooperation of Richard McKinley and the Air Force Research Laboratory. The test facilities were supported by Naval Air Engineering Station Lakehurst and the Joint Strike Fighter Program Office. A. A. Atchley and T. B. Gabrielson are supported by the Office of Naval Research. K. L. Gee and V. W. Sparrow are supported by the Strategic Environmental Research and Development Program and Wyle Laboratories.

References

[1]Gurbatov, S. N. and Rudenko, O. V. , "Statistical Phenomena," in *Nonlinear Acoustics*, edited by M. F. Hamilton and D. T. Blackstock, Academic Press, San Diego, 1998, Chapter 13.

[2]Crighton, D. G., and Bashforth, S. "Nonlinear Propagation of Broadband Jet Noise," AIAA 6th Aeroacoustics Conference, 1980, AIAA-80-1039.

[3]Morfey, C. L. and Howell, G. P., "Nonlinear Propagation of Aircraft Noise in the Atmosphere," *AIAA Journal*, Vol. 19, No. 8, 1981, pp. 986-992.

[4]Howell, G. P., "Nonlinear Propagation of Aircraft Noise in the Atmosphere," Ph.D. Thesis, University of Southampton, UK, 1983.

[5]Ffowcs Williams, J. E., Simson, J., and Virchis, V. J., "Crackle: an Annoying Component of Jet Noise," *Journal of Fluid Mechanics*, Vol. 71, No. 2, 1975, pp. 251-271.

[6]Krothapalli, A., Venkatakrishnan, L., and Lourenco, L., "Crackle: a Dominant Component of Supersonic Jet Mixing noise," 6th AIAA/CEAS Aeroacoustics Conference, 2000, AIAA-2000-2024.

[7]Bass, H. E., Sutherland, L. C., Zuckerwar, A. J., Blackstock, D. T., and Hester, D. M., "Atmospheric Absorption of Sound: Further Developments," *Journal of the Acoustical Society of America*, Vol. 97, No. 1, 1995, pp. 680-683.

[8]Bass, H. E., Sutherland, L. C., Zuckerwar, A. J., Blackstock, D. T., and Hester, D. M., "Erratum: Atmospheric Absorption of Sound: Further Developments," *Journal of the Acoustical Society of America*, Vol. 99, No. 2, 1996, p. 1259.

[9]McInerny, S. A. and Olcmen, S. M., "High-intensity Rocket Noise: Nonlinear Propagation, Atmospheric Absorption, and Characterization," *Journal of the Acoustical Society of America*, submitted for publication, 2003.

[10]Menounou, P. and Blackstock, D. T., "A New Method to Predict the Evolution of the Power Spectral Density for a Finite-amplitude Sound Wave," *Journal of the Acoustical Society of America*, Vol. 115, No. 2, 2004, pp. 567-580.

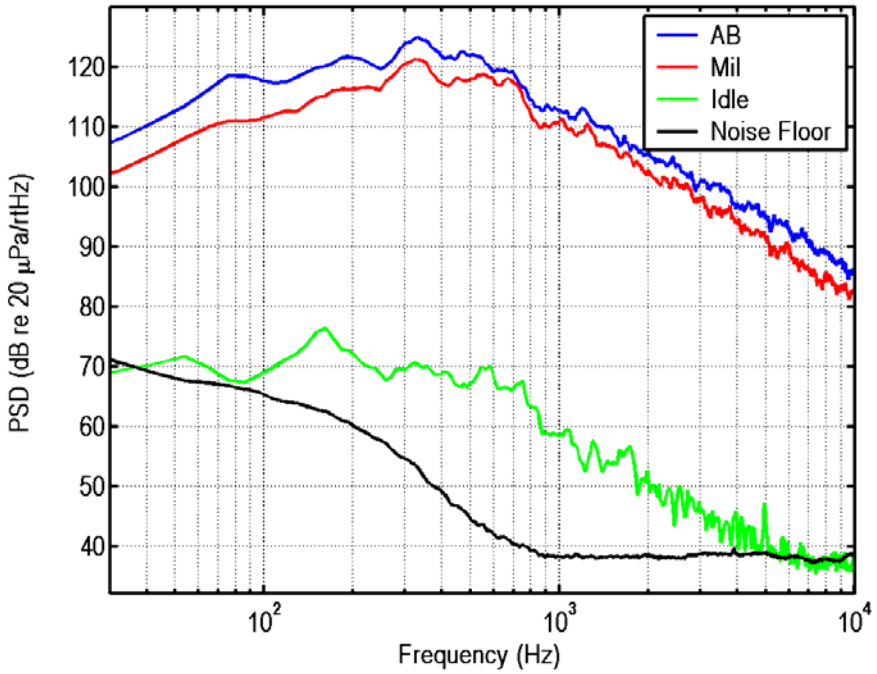

Figure 1: Power Spectral Density (PSD), in dB re 20 µPa/$\sqrt{\text{Hz}}$, at 18 m. The OASPL of the spectra at AB, Mil, and Idle are 151, 147, and 99 dB re 20 µPa, respectively.

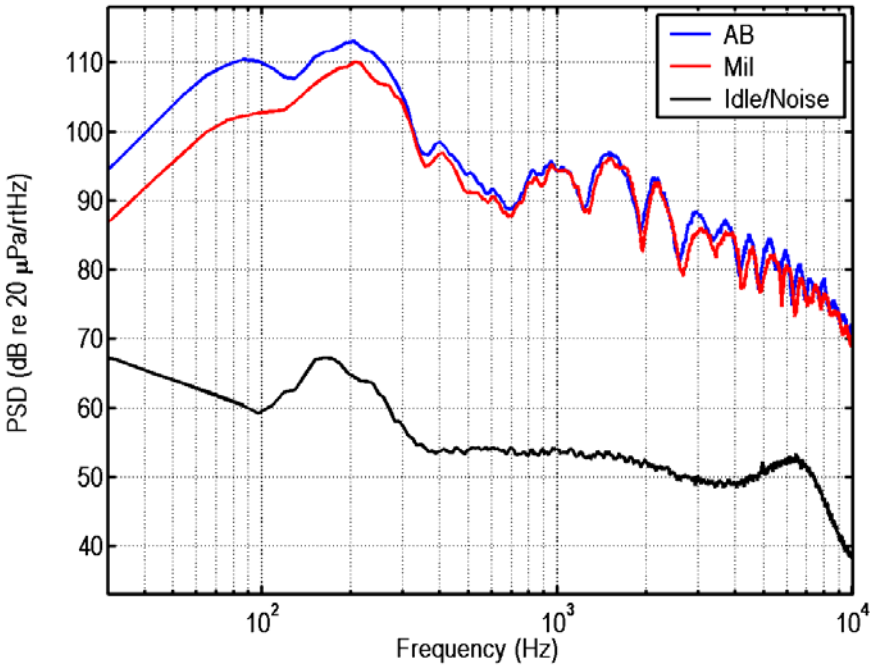

Figure 2: PSD at 74 m for the measured engine conditions. The OASPL of the spectra at AB and Mil are 135 and 132 dB re 20 µPa, respectively. The OASPL for Idle was not calculated because it largely falls below the system noise floor.

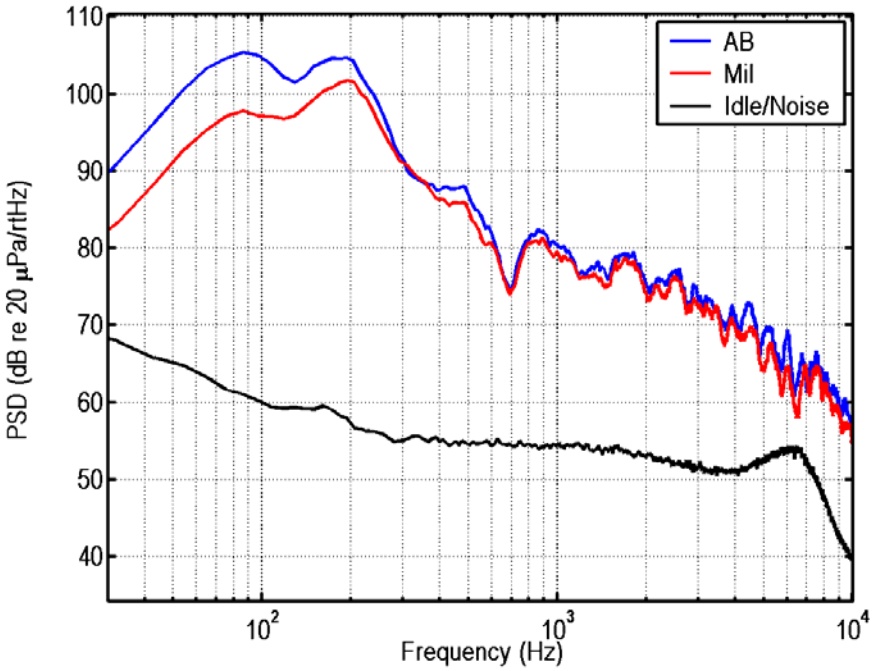

Figure 3: PSD at 150 m for the measured engine conditions. The OASPL for AB and Mil are 127 and 123 dB re 20 µPa, respectively. The Idle measurement levels are below the system noise floor.

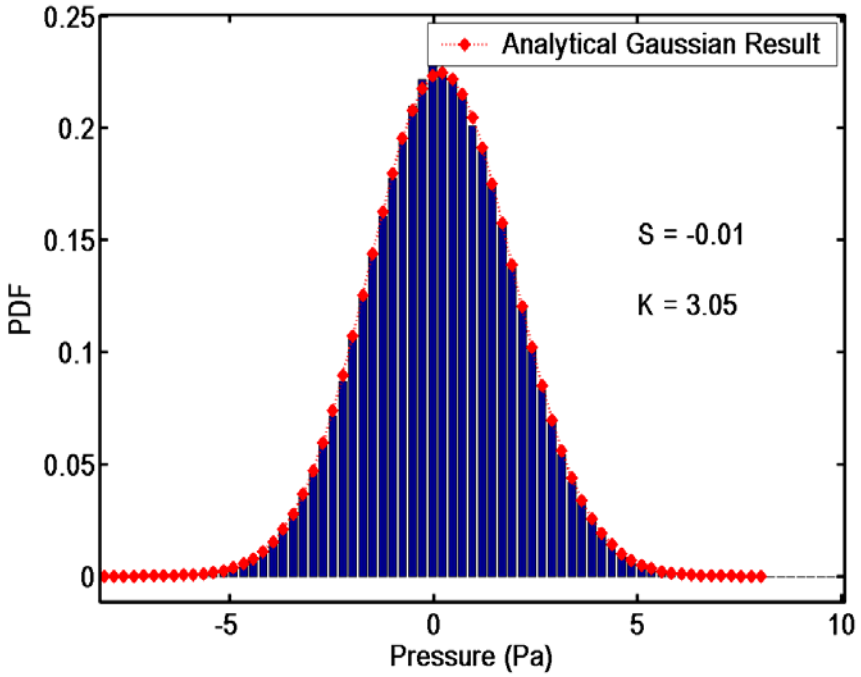

Figure 4: Probability density function (PDF), in blue, for the lowpass-filtered waveform (6 kHz cutoff) at 18 m with idle setting. The calculated PDF matches very closely the analytical PDF for a waveform with Gaussian statistics, shown in red.

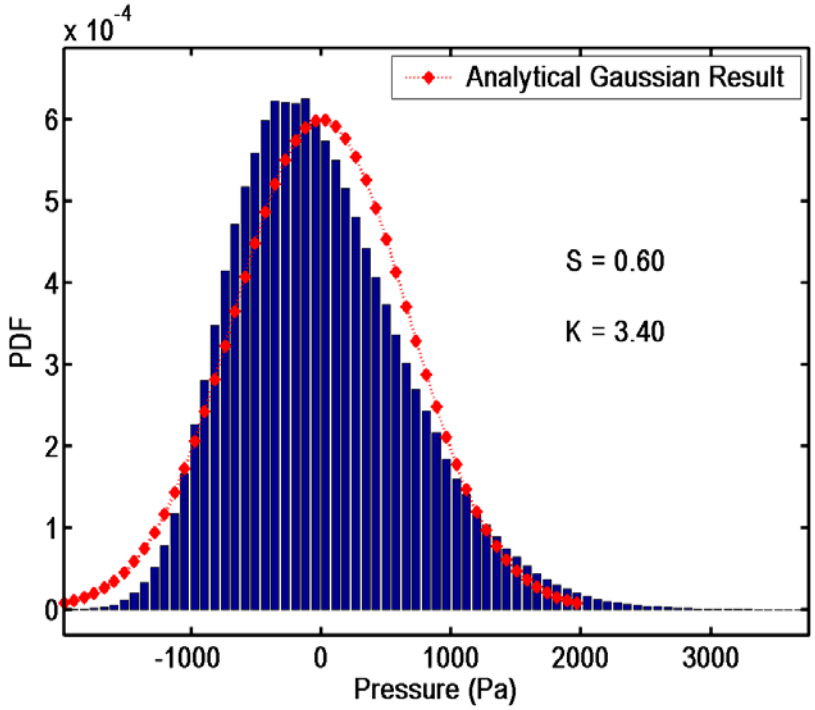

Figure 5: The PDF for the lowpass-filtered (10 kHz cutoff) waveform at 18 m for the AB case.

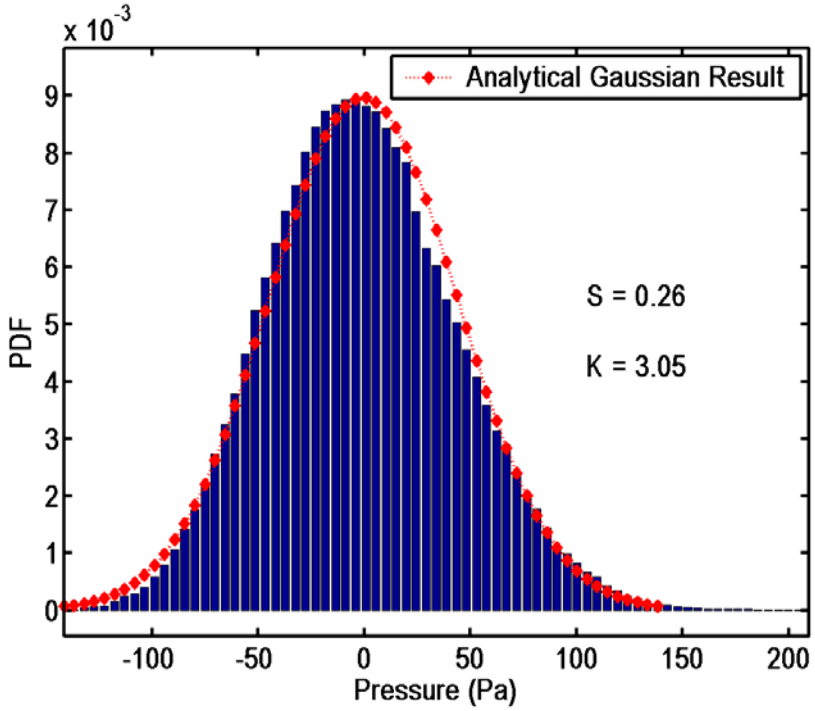

Figure 6: The PDF for the lowpass-filtered (10 kHz cutoff) waveform at 150 m for the AB case. The skewness (S) and kurtosis (K) are both less than in Fig. 5.

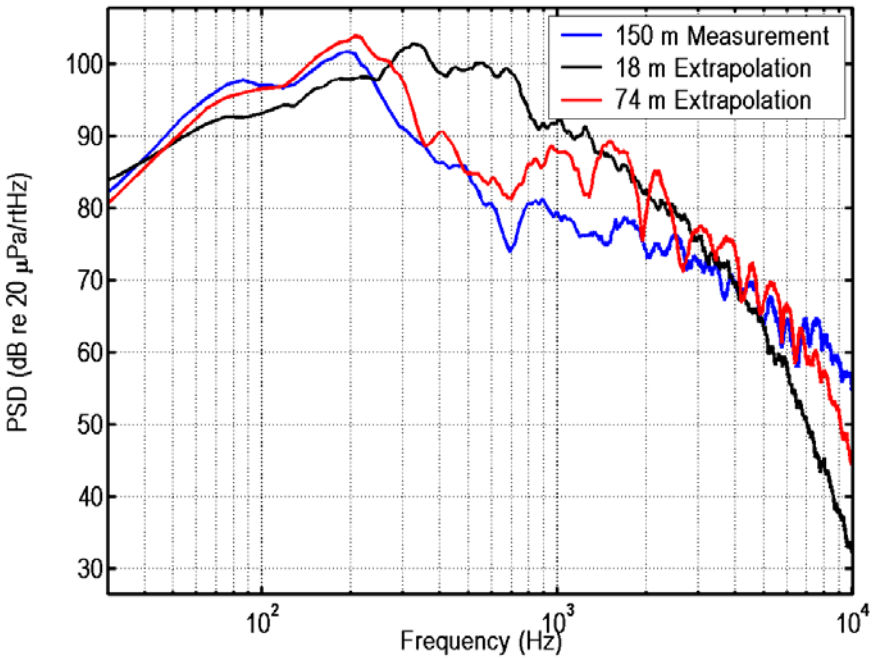

Figure 7: Comparison of linearly extrapolated spectra from 18 and 74 m with the 150 m Mil power measurement.

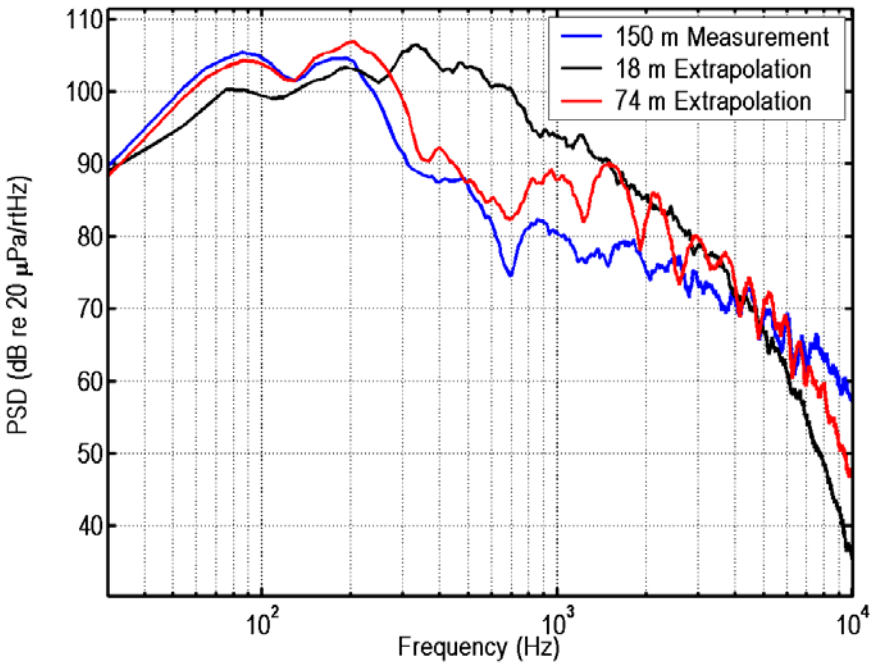

Figure 8: Comparison of linearly extrapolated spectra from 18 and 74 m with the 150 m AB measurement.

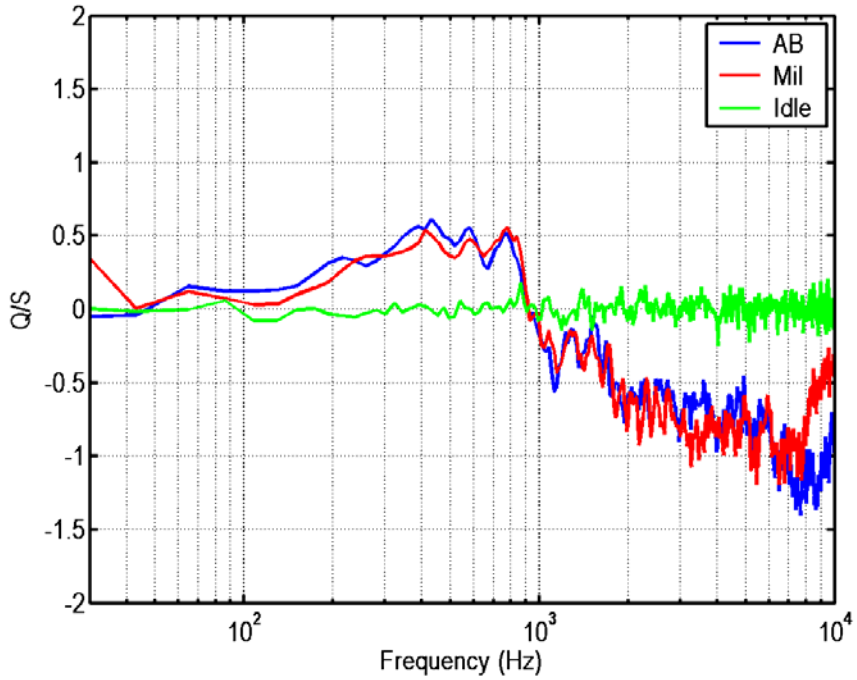

Figure 9: Howell-Morfey nonlinearity indicator, *Q/S*, calculated for the three engine conditions at 18 m. Note that the Idle calculation is only physically significant below 6 kHz, where the measured levels are above the system noise floor.

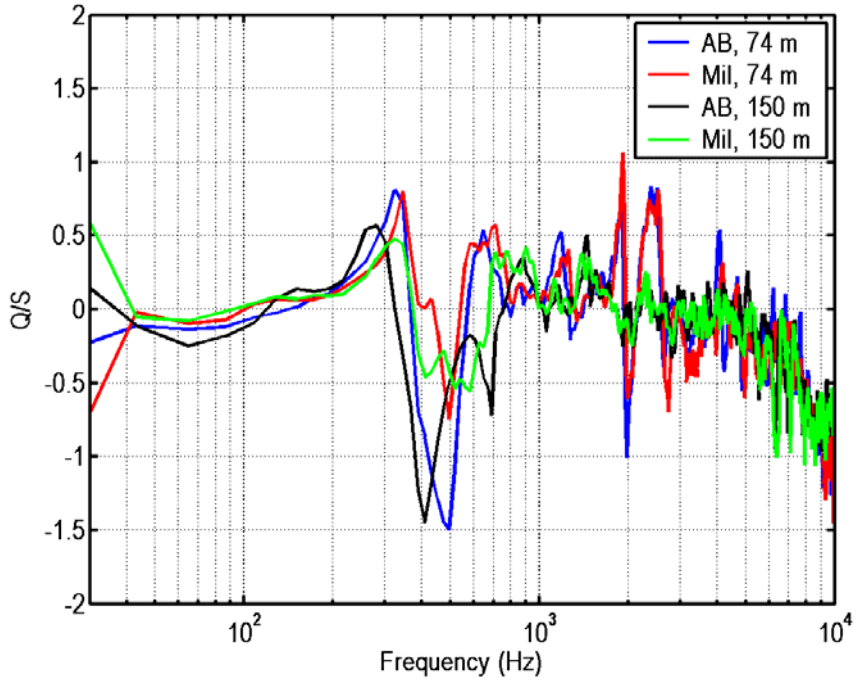

Figure 10: Howell-Morfey nonlinearity indicator, *Q/S*, at 74 and 150 m. The large peaks and sharp sign changes appear to be related to the spectral dips evident in the PSD measurements.

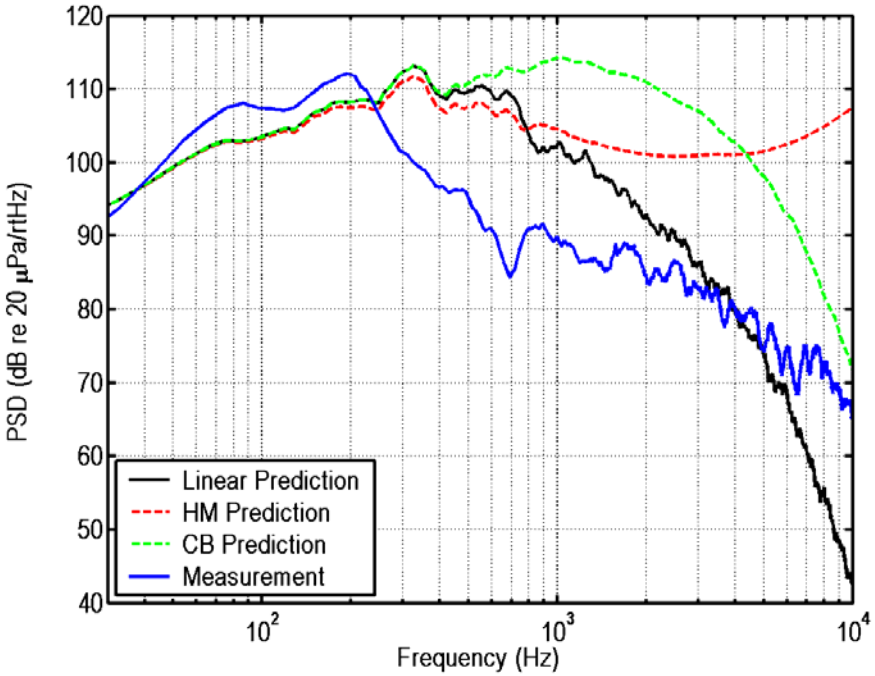

Figure 11: Comparison of the 150 m PSD measurement against the linear, Crighton-Bashforth (CB), and Howell-Morfey (HM) predictions for an input range of 18 m.

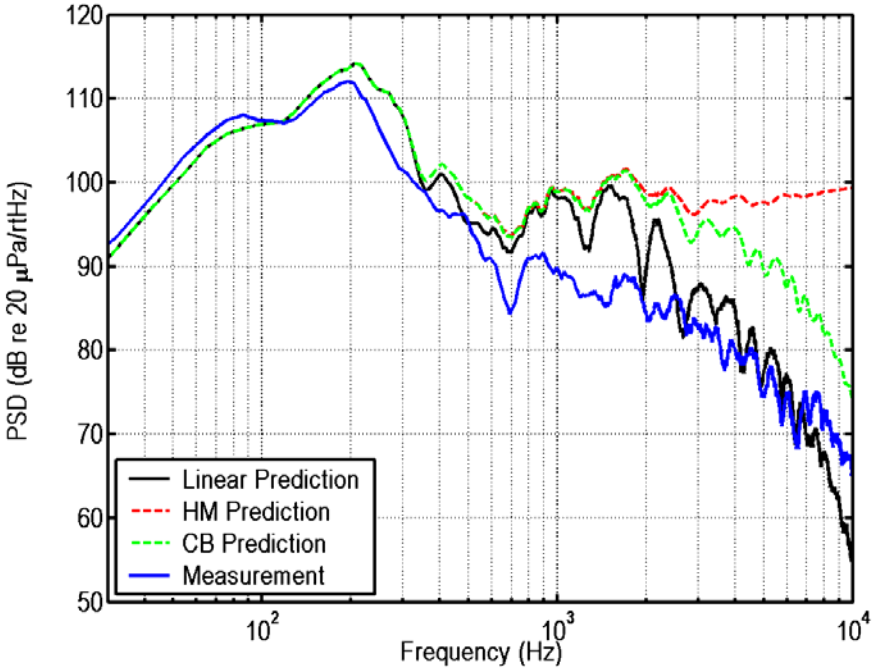

Figure 12: Comparison of the 150 m PSD measurement against the linear, CB, and HM predictions for an input range of 74 m.